COMPARISON OF DISPERSION DESCRIBED BY TRACER TESTS AND NMR PROPAGATORS USING THE SMIM MODEL.

M. Fleury[1], S. Stona[1], D. Bauer[1], M.C. Neel[2]

[1]IFP Energies nouvelles, Rueil-Malmaison, France
[2]Université d'Avignon et des Pays de Vaucluse

This paper was prepared for presentation at the International Symposium of the Society of Core Analysts held in Vienna, Austria, 27 August – 1 September 2017

ABSTRACT

Dispersion in porous media has been studied for a long time from breakthrough curves using a tracer. The NMR propagator technique is an alternate way for deriving dispersion from local velocimetry. In this work we compare the results obtained with both techniques on model porous media. Tracer tests were performed on homogeneous and heterogeneous grain packs using potassium iodium as a passive tracer detected at the outlet by a UV detector. On the same columns, NMR propagators were measured at different flow-rates for the same conditions

The data were analyzed using a general model called SMIM partially developed previously. With 4 parameters in addition to the dispersion coefficient, the model is able to reproduce two important features in dispersion: delayed breakthrough in dual porosity systems for example, and early breakthrough in the presence of preferential paths. For the analysis of NMR data, the SMIM model is described using analytical expressions reproducing directly the NMR signals, whereas for the tracer data, a numerical simulation is needed to calculate the breakthrough curve. NMR data were inverted to obtain the different dispersion parameters and then the breakthrough curves calculated and compared to measurements. Both techniques give comparable results; detailed discrepancies and limitations/advantages of the NMR approach are discussed.

INTRODUCTION

Dispersion in porous media has been studied for a long time from breakthrough curves (BTC) using a tracer [1]. Typically, one monitors at the outlet of a porous medium the spreading of a spike of tracer (a miscible fluid) injected at the inlet. In the simplest case (normal dispersion), the concentration vs. time curve is Gaussian and analyzed using an advection-dispersion equation (ADE) to obtain a dispersion coefficient D. It is well known that such approach is limited to homogeneous porous media and difficulties to analyse non-symmetric curves has long been recognized [2]. When more advanced models are used to reproduce for example trapping mechanisms in non-flowing porosity

fraction, or fast flow in preferential pathways, a single BTC is not sufficient and more information is required such as the spatial evolution of the BTC measured using local concentration along the core length [3]. The Pulsed Field Gradient (PFG) NMR technique is an alternate and much more direct method since the distribution of molecule displacements (propagator) is measured, and this is a unique information at the origin of dispersion mechanisms. Indeed the variance (or second moment) of the measured distribution is directly linked to the dispersion coefficient D without any assumption. This property has been used by many authors and results from both tracer and NMR methods gives comparable results (see Seymour et al. [4] for a compilation of results), although NMR tend to give lower D values. This simple approach does not apply in porous media with a complex structure such as double porosity carbonates [3], or in two phase flows performed in homogeneous systems [5]. When dispersion is anomalous, D will vary as a function of time as observed in NMR experiments [5], and for tracer experiments, a single value of D cannot be found when the length of the porous media is varied (i.e. D depend on space [3]). Hence models can truly be tested when appropriate experimental information is available and the final goal is to characterize a porous media with a unique set of parameters valid at all times and all locations.

In this work, we propose to test a new model (SMIM an acronym for Stochastic Mobile Immobile Model [6]) in a system containing important non flowing zones. In essence, the concepts in this model are not new and stochastic models such as CTRW (Continuous Time Random Walk [1]) are also able to reproduce similar physical mechanisms with the help of numerical simulations. However, the availability of analytical expressions for deriving the NMR signal allows inverting the model parameters in a very efficient way. The analytical expressions describe directly the NMR signal, and not its Fourier transform (propagator) avoiding some important difficulties. It uses also all the information contained in the signals, and not only the second moment that takes only into account the smallest wave numbers. Another objective of this work is to simulate the BTC and compare the results to measurements performed in the same porous media. For this purpose, a numerical simulator was developed to solve an equation applicable for a tracer (SMIMt).

THEORY

Dispersion from NMR data

The proposed model SMIM [6] is very general and attempts to reproduce two important mechanisms: (i) the possibility for a molecule to be temporarily trapped in non–flowing zones and (ii) the possibility for a molecule to travel large distances due to for example a highly contrasted velocity field. Hence, we reproduce deviations from the Gaussian case either by modifying the short or long displacement tails on both sides of the distribution. Empirical choices for representing these mechanisms were made: for the first mechanism, the well-known Mobile –Immobile concept is used [1,2], and for the second mechanism, the idea of Levy motions [7] is exploited with the important advantage that it includes the

Gaussian case. The complex PFG-NMR signal is given by the following analytical expressions [6]:

$$E(q,\Delta t) = < e^{-iq\Delta x} > = (F_- + GM)e^{r_-\Delta t} - (F_+ + GM)e^{r_+\Delta t} \quad (1)$$

where:

$$F_\pm = \frac{\eta}{K+1}\frac{A_\pm}{r_\pm} \quad G = \frac{K\eta}{K+1}\frac{1}{\sqrt{\Delta}} \qquad M = e^{-\omega(K+1)t_1} \qquad \eta = iqv_m + D|q|^\alpha\left[1+\tan\frac{\pi\alpha}{2}sign(q)\right]$$

$$2r_\pm = -(\eta+\omega(K+1)) \pm \sqrt{\Delta} \qquad A_\pm = \frac{\omega(K+1)-\eta}{2\sqrt{\Delta}} \pm \frac{1}{2} \qquad \Delta = \eta^2 + 2\eta\omega(K-1) + \omega^2(K+1)^2$$

where q is the NMR wave number (described later). The model has 5 parameters D, α, K, ω, v and an auxiliary parameter M with the following significance:

D: generalized dispersion coefficient [m^α/s],

α: stability exponent of the Levy distribution,

K: ratio of average immobile to mobile times,

ω: parameter describing the distribution of immobile times, exponentially distributed with a rate ω,

v_m: average velocity while moving (thus larger than the measured average velocity <v>), v=<v>(1+K),

M: a parameter describing memory effects.

These parameters are better understood when considering the corresponding dispersion equation below describing tracer tests.

Dispersion from tracer tests

The partial differential equation describing tracer experiments and corresponding to the SMIM model is the following:

$$\frac{\partial C}{\partial t} + K\omega e^{-\omega t} * \frac{\partial C}{\partial t} = -v\frac{\partial C}{\partial x} - D\frac{1}{\cos(\pi\alpha/2)}\frac{\partial^\alpha C}{\partial x^\alpha} \quad (2)$$

The parameter α is present in the fractional derivative of order α (definition given in [6]), and the trapping mechanism is identified by a supplementary term in the time derivative (the symbol * indicates a convolution). When α=2 and K=0, equation 2 corresponds to the standard ADE. This equation has been solved numerically by using a finite difference scheme of order 2. To properly represent diffusion, an operator splitting technique has been used. The calculation are made by introducing an initial Dirac impulse and integrating the curve to represent a stepwise continuous injection of tracer. Boundary conditions are more crucial. At the inlet of the column, the computation domain has been slightly augmented by a very small (0.02cm) transition zone in which the diffusivity smoothly decreases from D down to zero. For the present diffusivity and velocity values, this condition has no influence on the results. At the outlet and to avoid numerical perturbations, the computation domain has also been taken larger than in the experiments: homogeneous Dirichlet boundary condition has been imposed 4 cm after the physical outlet where break-through curves are recorded.

MATERIAL and METHODS

Porous media

A homogeneous pack was first prepared using well sorted glass beads with sizes in a narrow range [50 – 70 µm]. For this system, a porosity of 36.0% and a permeability of 2390 mD were obtained (length of the pack 27.73cm, inner diameter 2.40 cm). A second heterogeneous system was built by crushing a heavily micritized wackestone from the Eastern Paris basin (labeled GUD in Vincent et al. [8]). Before crushing, the bloc had a porosity of 22.7% and a permeability of 0.45 mD. The grains were sorted in the range [30-125 µm]. The porosity of the grain pack is 50.1%, composed of an inter-granular and intra-granular porosity respectively of 38.5% and 11.6%. The permeability of this heterogeneous system is 2380 mD (length 20.46 cm, inner diameter 2.40 cm).

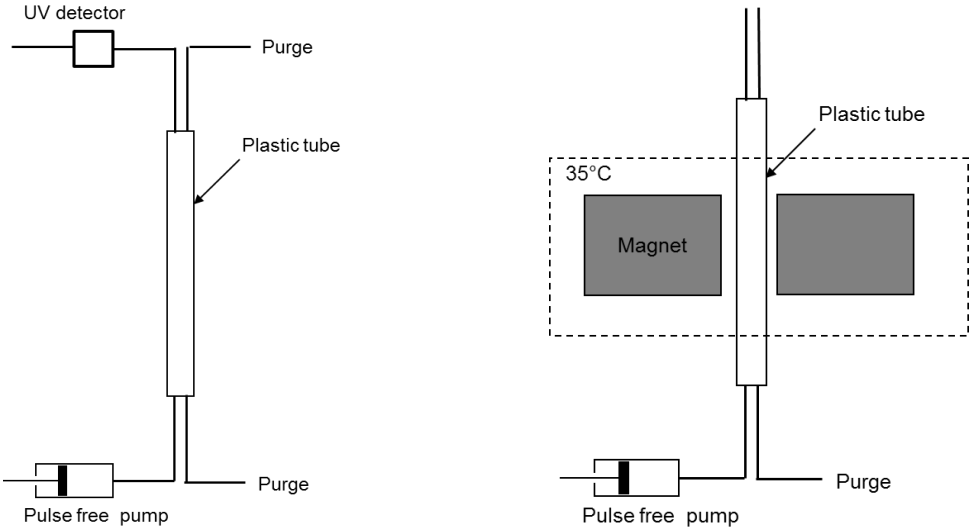

Figure 1: Experimental set-up for measuring breakthrough curves (left) and propagators in the NMR device (right). The column has an outer diameter of 30mm and a length up to 27 cm.

Propagator measurements

To perform propagator measurements (i.e. a measure of the spin bearing molecule displacement distribution in a given volume), the grain pack tube was placed in a 20MHz Oxford Instrument imaging system (Figure 1). The sequence used to measure displacement distributions is a bipolar pulsed field gradient stimulated echo sequence with z-storage in which a slice selection has been inserted to select a given volume in the column (Figure 2, more details are given in Guillon et al. [5]). To build the NMR signal E(q,t) and the displacement distribution for a given observation time t, echo amplitudes are collected for different values of the wave number q defined as :

$$q = \frac{\gamma g_{max} \delta}{2} \qquad P(\xi, t) = \int_{-\infty}^{+\infty} E(q,t) e^{i2\pi q\xi} dq \qquad (3)$$

where g_{max} is the maximum amplitude of the gradient pulse, and γ the proton giromagnetic ratio ($\gamma/2\pi$=42.58 MHz/T). The factor of 2 in the q calculation originates from the gradient shape. The gradient amplitude g_{max} was varied in 42 steps adequately spaced up to the noise level depending on the time t and injection velocity.

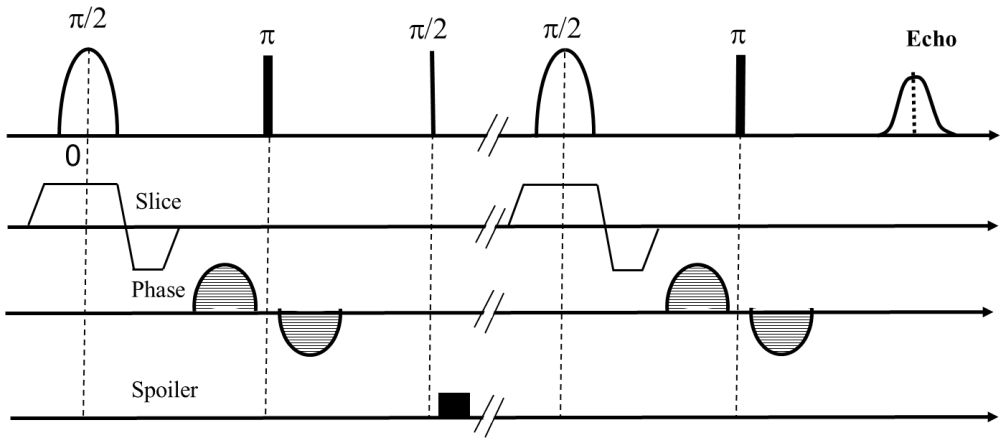

Figure 2: NMR sequence for measuring propagators, 20 MHz Oxford Instrument imaging system. The sequence comprises essentially a slice selection (2 cm thickness) and a bipolar phase encoding performed along the flow direction.

Dispersion can be evaluated from NMR propagator measurements providing (i) the mean displacement is much larger than the grain size ($\langle \xi \rangle > 5d_g$ [5,9]) (ii) the molecular diffusion is large enough to allow particles to probe several streamlines (criterion $L_d = \sqrt{2D_m t} > 0.3d_g$ where D_m is molecular diffusion [9]). Thus, the first criteria requires that <v>t be large enough; in practice, depending on the mean velocity, observation time above 200 or 500 ms are required. With such values, the second criteria is also met. Furthermore, in the context of the SMIM model, it is the time dependence of the propagator that allows determining the numerous parameters of the model, and not only one measurement at a single time. Hence, usually 4 measurements were performed at times varying from 500 up to 1400 ms. We verified that 4 measurements are enough to obtain the desired information by performing one experiment with 16 times varying from 500 up to 2000 ms. We also verified for each experiment that the mean velocity measured by NMR is coherent within experimental uncertainties with the mean velocity deduced from the imposed flow rate and porosity. This implies also that the gradient amplitudes are properly calibrated yielding accurate dispersion coefficients.

For the homogeneous system with a single longitudinal or transverse relaxation time, NMR measurements were performed with the column fully saturated with water and observation time t varying from 500 ms up to 1000 ms. For the bimodal system saturated

with water, the transverse relaxation time is non-unique and has two peaks (T_2=300 and 35 ms) corresponding respectively to the inter and intra-granular porosity. Hence, when large observation times are used (200 ms and more), the displacements inside the grains cannot be detected because the magnetization originating from this porosity fraction has relaxed to zero . Hence, we saturated this porous medium with cyclohexane, a non-polar molecule with very weak surface interaction; as a result, a single relaxation time is observed at about 700 ms, allowing propagator experiments to detect without bias the displacements in the entire pore volume. This is a key issue in many non-strictly homogeneous natural porous media in which there is a relaxation time distribution generating a T_1 or T_2 weighted propagator [10].

Tracer measurements

Using the same porous media, breakthrough curves were measured using a water solution containing 20 ppm of potassium iodure (KI). The concentration of this tracer is then detected by a UV detector at a wavelength of 226 nm (Figure 1). We checked that the response of the detector as a function of the KI concentration is accurate and linear. The detector is placed as close as possible to the outlet of the cell (a few cm). To minimize the dispersion effects close to the inlet and outlet, the inlet and outlet end-pieces, equipped with two tubings, are first saturated with the KI solution, while the grain pack is fully saturated with (pure) water. Then the KI solution is continuously injected and the data acquisition started. As a result, the recorded signal shows several phases (Figure 3): (i) the KI solution contained in the tubing connecting the outlet to the UV detector is first detected; the absorbance decreases from a maximum down to zero (ii) the water inside the porous media is detected; absorbance is zero until (iii) the injected KI solution is detected; the signal increases from zero up to a maximum. After normalization of the curve by the largest absorbance (i.e. the curve varies from 0 to 1, 1 being the 100% tracer concentration relative to the injected solution), a time origin is defined as the time at which the tracer concentration is equal to 0.5 during phase 1. Hence, the time shift between the outlet and the detector is taken into account. In a similar way, injecting pure water after the sequence described above also provides a breakthrough curve. Hence, several experiments could be repeated.

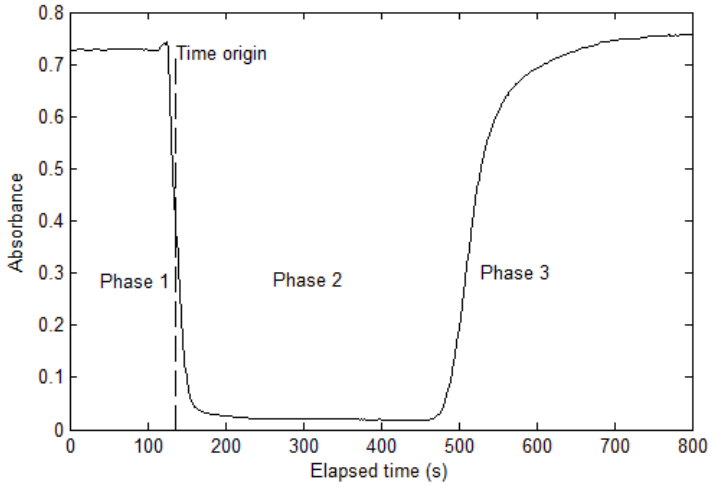

Figure 3: Typical aspect of a recorded signal when measuring breakthrough curves.

RESULTS

The general approach is to determine the dispersion properties from NMR measurements and the SMIM model. Then the same parameters are utilized in the tracer model SMIMt to predict a breakthrough curve. This curve is then compared to the tracer measurement. We present the results and comparisons for the two grain packs below. Four injection flow rates were used varying from 600 up to 1200 ml/h. Peclet numbers Pe vary between 20 and 40 ($Pe = vl/D_m$ where D_m is the molecular diffusion coefficient of water at 30°C, 2.6 10^{-5} cm^2/s, l is taken as the mean bead diameter).

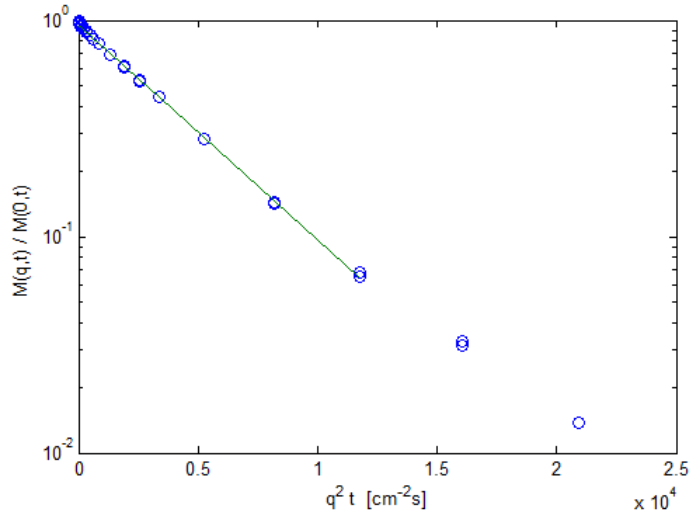

Figure 4: Example of the determination of the dispersion coefficient for the glass bead pack. Flow rate 800ml/h (<v>=0.136 cm/s), observation time t=599.4 ms. The slope D is 2.28 10^{-4} cm^2/s. The last two points not taken in the fitting are influenced by noise.

Homogeneous bead pack

For this system, we observed that the propagators are Gaussian. Indeed, when the magnetization is plotted vs. q^2t, a single exponential decay can be fitted (Figure 4) down to the noise level. Hence, the dispersion coefficient can be determined in a simple way according to :

$$\ln\left[\frac{M(q,t)}{M(0,t)}\right] = -Dq^2t \tag{4}$$

The Gaussian case is one particular case of the SMIM model (α=2, all other coefficients K, ω, M equal to zero). For each flow rate, we determined a dispersion coefficient D (Table 1) as an average of the coefficient measured as a function of time (6 values from 500 up to 1000 ms). Indeed, D does not depend on time within experimental uncertainties (Table 1). As expected, D increases with the pore velocity or Peclet number. The dispersivity D/v expected to be constant increases however slightly with the pore velocity from 16 up to 19 µm.

The measured and simulated breakthrough curves are shown in Figure 5. The measured curves are much larger than the simulated ones. We indicate also as a guide the analytical solution of the ADE taking a dispersivity equal to the mean bead size (D/l=60 µm or D=8.2 10^{-4} cm^2/s). In this case, we cannot conclude about the coherency between NMR and tracer tests; with such a small dispersivity, small perturbations in the tracer tests are critical. Indeed, although the experimental set-up has been designed with the shortest distance between the outlet and detector, the measured breakthrough curves are not symmetric due to dispersion occurring between the outlet and the detector. This aspect will be analyzed further in the section the Discussion section.

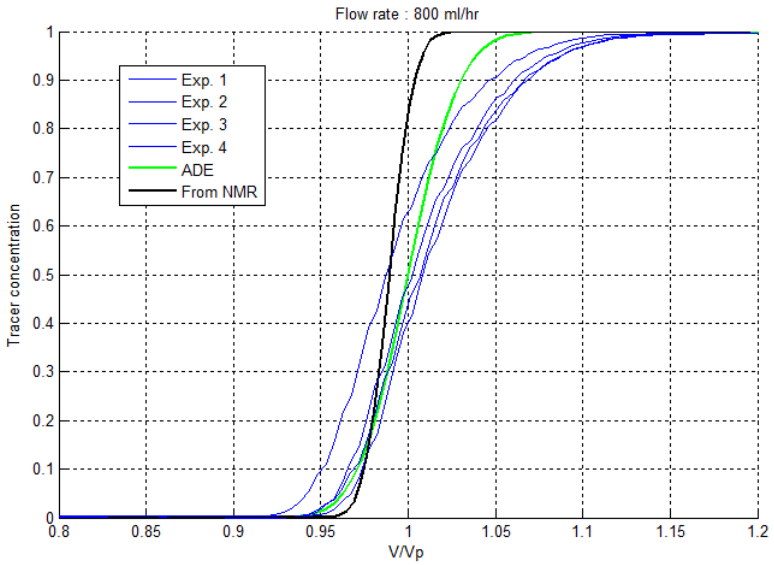

Figure 5: Measured breakthrough curves compared to simulations for the homogeneous bead pack.The blue curves are 4 repeated experiments, the green curve correspond to a standard ADE taking D=8.2 10^{-4} cm^2/s, the black curve corresponds to a simulation in which the NMR dispersion coefficient has been taken.

Bimodal grain pack

To obtain the parameters of the SMIM model, several E(q,t) signals were fitted simultaneously [6]. In most cases, 4 or 5 signals with observation time varying from 200-500 up to 1400 ms were used (Figure 6), yielding large average displacements, much larger than the mean grain size (Table 2). By fitting these signals for different α values spanning from 1.7 up to 2 [6], we found that the value yielding the lowest objective function was always close to 2 (from 1.90 up 1.98). Hence, it was decided to impose α=2 when inverting the SMIM parameters. Therefore, the SMIM model becomes a classical MIM model in which molecules can be trapped in non-flowing zones, and such model is presumably well suited for the present situation. The most interesting parameter is K, the ratio of immobile to mobile particles. For this system, we expect a ratio of the order of the ratio of intra to inter-granular porosity (11.6/38.5=0.30); we find indeed a value in the range [0.21-0.36], increasing with the mean velocity (Table 2). The dispersion coefficient increases with the mean velocity or Pe number, but the dispersivity is nearly stable (51±4 μm).

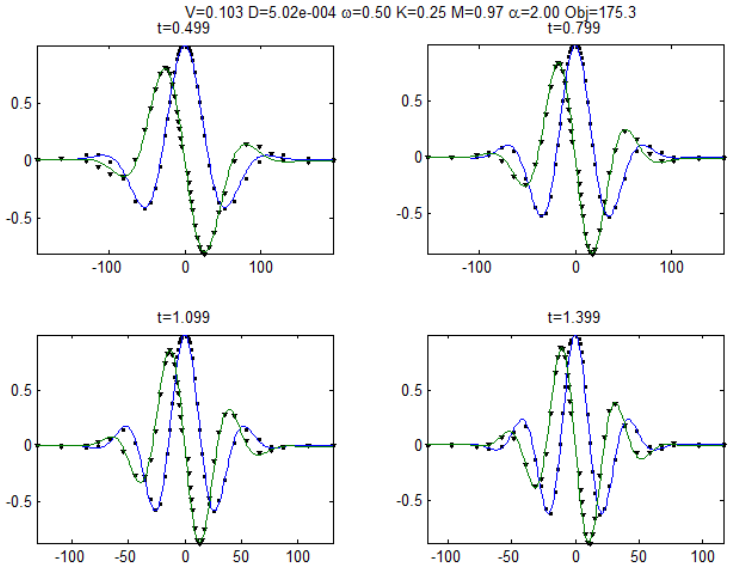

Figure 6: Real and imaginary E(q,t) NMR signals (square and triangle) fitted with the SMIM model (green and blue lines) for the heterogeneous bimodal grain pack. The observation times t are indicated in units of seconds. Flow rate: 800 ml/h. The resulting parameters are: D=5.02 10^{-4} cm^2/s, v_m=0.103 cm/s, K=0.25, ω=0.50, M=0.97.

The comparison between the simulated and measured breakthrough curves is also very instructive (Figure 7 for a flow rate of 800 ml/h). Although the agreement is not perfect, we see clearly that the model in which we used the parameters determined from NMR measurement is able to reproduce the early breakthrough at V/Vp~0.8 and a slight asymmetric shape. The asymmetry is more pronounced for the measured curves. The results obtained for other flow rates are all similar to this one. To obtain a physically sound result, the simulated curves were not scaled by the pore volume but by the volume in which particles are moving (V_p/(1+K)).

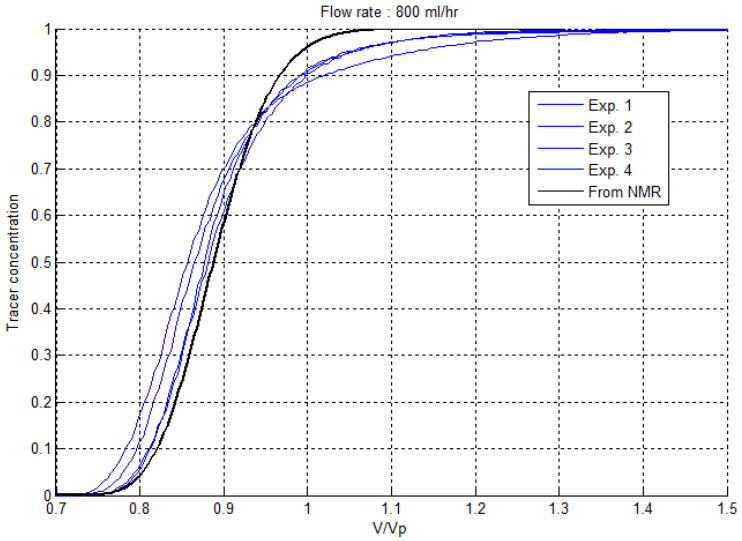

Figure 7: Comparison of simulated and measured breakthrough curves for the heterogeneous bimodal grain pack.

DISCUSSION

The direct use of the NMR signals in the inversion process is very important numerically; however, they have no direct physical meaning. Here, we compare the propagators obtained from the NMR signal in the bead pack and the grain pack for the same pore velocity (about 0.1 cm/s) and two observation times (Figure 8). For the bimodal grain pack, there exist a tail at zero or negative velocities, whereas this is not the case for the homogeneous bead pack. This tail subsist even at large observation times (1400 ms). This is actually the information provided by the signals and used to find the existence of a certain porosity fraction in which little or no flow is occurring (parameter K~0.3 in agreement with micro-porosity fraction in this system). Surprisingly, the propagator for the bimodal grain pack does not show a distinctive peak around zero velocities; this means that the exchange between the intra and inter-granular porosity due to molecular diffusion has a time scale shorter than the observation time. For this system, the micro-porosity is well connected to the macro-porosity.

The agreement between the BTC calculated from NMR data and the measurements is convincing for the bimodal grain pack, but not for the homogeneous bead pack. One source of discrepancy is that the NMR is a local measurement performed over about only 10% of the column, whereas the tracer experiment is valid for the entire column in which small packing defects can accumulate. But the most important aspect is that the tracer experiment has a limited resolution in terms of dispersion coefficient compared to NMR. Indeed, the dispersion of the tubing connecting the outlet face of the sample to the detector, even reduced to a minimum, has a large impact; a 1/8” or 1/16” tubing of a few centimeter with an inner diameter 10 or 100 times larger than the grain size can have a similar dispersion as the entire column only about 5 times longer. The applied protocol can give some information about these effects. Indeed, for each experiment, the

dispersion of the outlet line is measured in order to set the time origin (Figure 3); therefore the width of the BTC cannot be smaller than the width of this early signal. Indeed, for the homogeneous bead pack, we observed that the slope estimated at a concentration C=0.5 characterizing the outlet line and later the porous media are nearly identical. Thus, the tracer experimental device as designed in these experiments is capable of determining dispersivity only larger than about 60 μm, whereas NMR has no limitation and can characterize motions down to molecular diffusion.

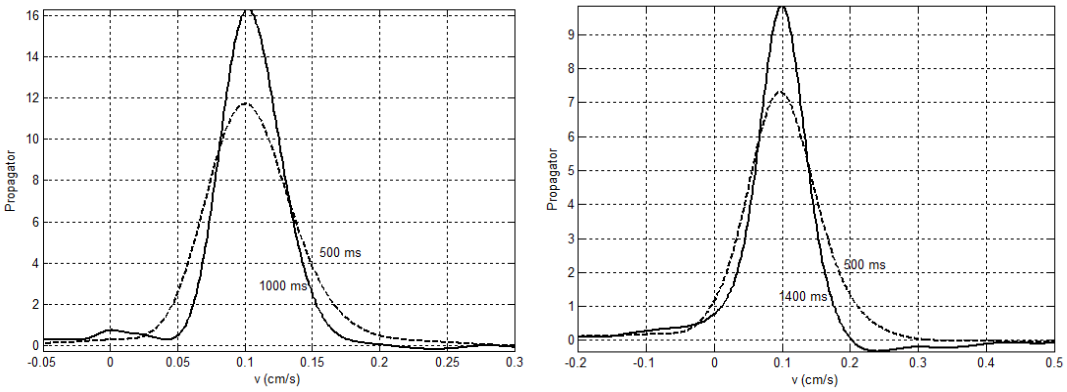

Figure 8: Propagators calculated for the homogeneous bead pack (left, Q=600ml/h) and the bimodal grain pack (right, Q=800 ml/h).

CONCLUSION

For two model systems, we performed NMR propagator and tracer measurements in order to compare the NMR prediction on the shape and position of the breakthrough curve (BTC). The NMR analysis is performed using a model (SMIM) able to reproduce the most important features in dispersion: (i) trapping mechanisms in non- flowing zones and (ii) preferential pathways. The BTC are simulated using a numerical model taking as input the parameters determined in the NMR experiments. In this study, we tested the case of non- flowing zones by packing a bimodal system made of porous grains obtained by crushing a carbonate system of known porosity and permeability.

The results show that the early breakthrough observed on the BTC in the bimodal system is well reproduced by the NMR prediction. Furthermore, the NMR model used to interpret propagators also predicts a non-flowing porosity fraction in agreement with the intra-granular porosity. For the homogeneous case, the NMR dispersivity is smaller than the one deduced from BTC due to the important and unavoidable effect of outlet line dispersion.

Table 1: Results of NMR measurements for the homogeneous beak pack. Mean bead size: 60 µm. . $<l_D>$ is the range of mean displacement for a given flow rate (<v>t), <*v*> is the average velocity.

Flow rate (ml/h)	<*v*> (cm/s)	$<l_D>$ (µm)	D *10^4 (cm^2/s)	Dispersivity (µm)	Pe
600	0.102	510-1020	1.62±0.03	15.9	23.5
800	0.136	680-1360	2.36±0.02	17.4	31.4
1000	0.170	850-1700	3.08±0.02	18.1	39.2
1200	0.204	408-2243	3.90±0.04	19.1	47.1

Table 2: Results of NMR measurements for the heterogeneous bimodal grain pack. Mean grain size: 75 µm. $<l_D>$ is the range of mean displacement for a given flow rate (<v>t), <*v*> is the average velocity.

Flow rate (ml/h)	<*v*> (cm/s)	$<l_D>$ (µm)	D *10^4 (cm^2/s)	*D/v* (µm)	v_m (cm/s)	K	ω (1/s)	M	Pe
600	0.074	366-1024	3.53	47.5	0.077	0.21	0.50	1.00	21.4
800	0.098	488-1366	5.02	51.4	0.103	0.25	0.50	0.97	28.2
1000	0.119	244-1708	6.03	50.5	0.129	0.30	0.78	0.98	34.5
1200	0.143	293-2094	7.86	55.0	0.154	0.36	0.70	0.98	41.3

References

[1] M. Sahimi, Flow and Transport in Porous Media and Fractured Rock, Wiley-VCH, 2011.

[2] K. H. Coats and B. D. Smith, Dead-end pore volume and dispersion in porous media, Soc. Pet. Eng. J. 73 (1964).

[3] M. Fourar, G. Radilla, Non-Fickian Description of Tracer Transport Through Heterogeneous Porous Media, Transport in Porous Media 80 (2009) 561–579.

[4] J.D. Seymour, P.T. Callaghan, Generalized approach to NMR analysis of flow and dispersion in porous media, AIChE Journal 43 (1997) 2096–2111.

[5] V. Guillon, M. Fleury, D. Bauer, Neel, M. C., Superdispersion in homogeneous unsaturated porous media using NMR propagators, Physical Review E 87 (2013) 043007.

[6] M.-C. Néel, D. Bauer, M. Fleury, Model to interpret pulsed-field-gradient NMR data including memory and superdispersion effects, Physical Review E 89 (2014) 062121.

[7] R. Metzler, J. Klafter, The random walks guide to anomalous diffusion: A fractional dynamics approach, Physics Reports 339 (2000) 1–77.

[8] B. Vincent, M. Fleury, Y. Santerre, B. Brigaud, NMR relaxation of neritic carbonates: An integrated petrophysical and petrographical approach, Journal of Applied Geophysics 74 (2011) 38–58.

[9] U.M. Scheven, P.N. Sen, Spatial and temporal coarse graining for dispersion in randomly packed spheres, Physical review letters 89 (2002) 254501.

[10] J. Mitchell, Graf von der Schulenburg, D. A., D.J. Holland, E.J. Fordham, M.L. Johns, L.F. Gladden, Determining NMR flow propagator moments in porous rocks without the influence of relaxation, Journal of Magnetic Resonance 193 (2008) 218–225.